RSC Advances

ROYAL SOCIETY OF CHEMISTRY

www.rsc.org/advances

Graphical Abstract

Preparation, modification and characterization of polymeric hollow fiber membranes for pressure retarded osmosis

Pravin G. Ingole, Kee Hong Kim, Chul Ho Park, Won Kil Choi, Hyung Keun Lee*

Greenhouse Gas Research Center, Korea Institute of Energy Research (KIER), 71-2 Jang-dong, Yuseong-gu, Daejeon-305343, Republic of Korea

*Corresponding author: Tel.: +82-42-860-3647

Email address: hklee@kier.re.kr (Hyung Keun Lee)

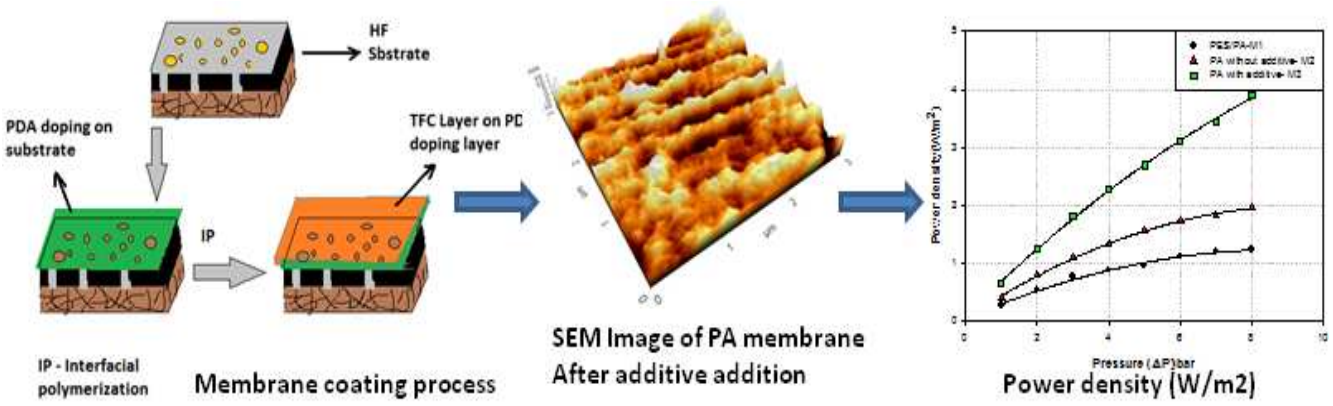

Cite this: DOI: 10.1039/c0xx00000x

www.rsc.org/xxxxxx

ARTICLE TYPE

Preparation, modification and characterization of polymeric hollow fiber membranes for pressure retarded osmosis

Pravin G. Ingole, Kee Hong Kim, Chul Ho Park, Won Kil Choi and Hyung-Keun Lee *

Received (in XXX, XXX) Xth XXXXXXXXX 20XX, Accepted Xth XXXXXXXXX 20XX
DOI: 10.1039/b000000x

The present study evaluated the performance of pressure retarded osmosis (PRO) process for power generation. This study systematically investigated to develop a high flux and high power density. The polyethersulfone (PES) membrane support was modified by coating with polydopamine (PDA). After polydopamine coating, the effect of additive during interfacial polymerization to make thin film composite (TFC) layer on polydopamine coated layer was studied. At the time of interfacial polymerization we added the tributyl phosphate (TBP) as an additive in the organic solution of monomer to increases the water flux and power density. The modified membranes were then well characterized by ATR-FTIR, SEM, AFM, TEM, porometry, contact angle and performance were evaluated by salt rejection, water permeability, and power density. The relationship between the performance of TBP additive and the physicochemical properties of the polyamide layers, that is, the free volume, surface roughness and hydrophilicity seemed very well. The experimental results indicated that addition of TBP additives on the retention properties of composite membrane is different; the certain concentration of TBP additives can be retained in the membrane properties of the same circumstances, so that membrane water flux along with power density increased.

1. Introduction

Increasing population, rising water demand and impairment and increasing demands of energy use over the past decades stimulated exploration of alternative water and energy resources. Emerging osmotically driven membrane processes might provide sustainable solutions for the global needs of both clean water and main important is clean energy.[1-7] Electricity is the fundamental energy source for civilized and industrial society. With increasing industrialization globally, the total energy consumption has increased by 6% annually which is supplied by MW-sized power plants using hydroelectric, nuclear, and thermoelectric power. However, these technologies are associated with environmental challenges such as CO_2 emissions, radioactive contamination, and climate change. Accordingly, many countries have been developing and exploring various clean renewable energy technologies, e.g., photovoltaic, solar heat, wind, and ocean thermal energy conversion. Electricity must be supplied continuously to avoid blackouts under forecast loads. Therefore, it is not possible for current renewable energies to serve as the primary electricity supply due to limitations in operating times which occurs due to location, temperature and weather. Power generation by using pressure retarded osmosis (PRO) offers the possibility for developing osmotic pressure gradients for a wide range of applications. PRO is an emerging platform technology that has the potential to sustainably produce electric power.[8-10] Early PRO studies using asymmetric reverse osmosis (RO) membranes observed extremely low power density due to their thick support layers.[11-14] Recent developments regarding zeolites are also a good material for increasing the flux as well as useful in microsystems for chemical synthesis and energy generation.[15-19] Interfacial polymerization (IP) proved to be an excellent method to obtain a very thin active layer on a support membrane.[20,21] Since then, a lot of progress has been made in the field of osmotic membrane fabrication. Recently our group also fabricated and modified number of TFC membranes consisting of polyethersulfone porous substrates for energy generation.[22]

Polyether sulfone (PES) is a high-performance thermoplastic polymer with outstanding thermal stability, flame resistance and flexibility, widely used as a substrate for hollow fiber composite membranes.[23] Li et al successfully fabricated defect-free polymeric dual-layer hollow fiber membranes consisting of an ultrathin dense-selective polyamide imide (PAI) layer and a polyethersulfone (PES) supporting for gas separation application. It is observed that a lower outer-layer dope flow rate does not necessarily result in the formation of an ultrathin dense-selective layer upon the PES supporting layer.[24] Our group also has a good experience to fabricate and modified PES hollow fiber membranes for diverse applications like water vapor removal,[25] gas separation[26] etc. Rahimpour et al applied the asymmetric

polyethersulfone and thin-film composite polyamide nanofiltration membranes for water softening.[27] A number of commercial high-pressure nanofiltration membranes are asymmetric membranes without composite structure, such as NP010 and NP030 made by Nadir Corporation. The material of this membrane is also polyether sulfone.

PDA is a polymer with chemistry similar to the adhesive secretions of mussels.[28-30] It is formed from the spontaneous polymerization of dopamine in an alkaline aqueous solution. The polar groups in PDA layer, such as hydroxyl and amine groups, bequeath the substrates with improved hydrophilicity and anti-fouling ability.[31] A subsequent study using PDA modified membranes for osmotically driven membrane process was first done by Arena et al.[32] This was done through the application of PDA to TFC membrane support layer(s). Significant improvements in the water flux of PDA modified TFC PRO membranes were observed in the pressure retarded osmosis (PRO) orientation.[33]

We choose the PES hollow fiber membrane for PDA modification. Our study systematically investigated the effects of additive, effect of DA coating, effect of TFC on PDA coating, effect of coating times, effect of pressures on the membrane performance and PRO performance using self making PES hollow fiber membranes as substrate materials. As a consequence, this study may not only present a systematic investigation on the development of novel and well-constructed TFC hollow fiber membranes for PRO with enhanced power density through an IP concept and surface modification, but also provide useful insights and guidelines to design next-generation membranes for PRO applications.

2. Experimental

2.1. Materials

Polyethersulfone (PES, Ultrason® E6020P, BASF, Germany), used as the base polymer, was purchased from General Electric Company. N-methyl-2-pyrrolidion (NMP) with purity more than 99.5% was purchased from Merck and was used as solvent without further purification. Lithium chloride (LiCl, Sigma Aldrich) was used as pore former in dope solution. Dopamine, diamine monomers m-phenylenediamine (MPD) and piperazine (PIP), acid chloride monomer trimesoyl chloride (TMC) and tributyl phosphate (TBP) were purchased from Sigma-Aldrich. Hexane, the solvent for TMC, methanol were purchased from Fisher Scientific. Deionized water (DI) obtained from a Milli-Q ultrapure water purification system (Millipore) was used as the solvent for diamine monomers. Sodium chloride was purchased from Fisher Scientific.

2.2. Methods

2.2.1. Preparation of PES hollow fiber membrane

A PES hollow fiber membrane was fabricated using the dry/wet phase inversion method. PES has excellent thermal and dimensional stability as well as strong chemical resistance.[34] PES also has a high degree of chain rigidity because of its regular and polar backbone. The method to fabricate the hollow fiber membrane has been explained elsewhere.[35] In this present work, the dope solution and internal coagulant (D.I. water) were passed through a double pipe spinneret of 0.16/0.9 mm inner/outer diameter with an air gap maintained at 0.5 cm. The dope solution was composed of 18.0 wt.% PES (Ultrason® E6020P, BASF, Germany), and 77.0 wt.% N-methylpyrrolidone (NMP, Merck) and 5.0 wt.% lithium chloride (LiCl, Sigma Aldrich, USA) were used as the solvent and additive, respectively. Hollow fiber passed through the first coagulation bath where phase inversion occurred rapidly. After that, it moved to the second coagulation bath where hollow fiber was washed out and coiled around the winder. The as-spun fibers were rinsed in a water bath for six days to remove the remaining solvent. Then, fibers were post-treated with methanol for two hours to improve flux and were dried for six days. Fig. 1 represents the schematic diagram of hollow fiber membrane spinning system.

2.2.2. Preparation of membranes for dopamine coating on hollow fiber membrane

The PDA modification followed the procedure set forth in previous work.[28] Since the PDA formation only occurs in the aqueous phase. The newly prepared solution was shaken vigorously at 25 °C to avoid the formation of large PDA particles. The cleaned PES membranes were immersed in the solution of 2 mg/ml DA-HCl at pH 8.5 (PBS buffer). After desired time of polymerization (1 h), the coated membranes were washed with double distilled water for 24 h to remove the redundantly dark brown precipitates. Polymerization occurs at room temperature with non-agitated solutions exposed to the air. The PDA polymerization can be observed upon the addition of dopamine where the formation of PDA is indicated by the change in color of the polymerizing dopamine solution from clear to orange and finally to brown. The color of fiber is changed as shown in Fig. S1 (Supporting information Fig. S1).

2.2.3. Polyamide active layer fabrication

The thin film composite membrane was prepared by coating selective layer in situ on the surface of polydopamine coated hollow fiber membrane by interfacial polymerization of m-phenylenediamine (MPD) with trimesoyl chloride (TMC). The polydopamine coated hollow fiber membrane was immersed in an aqueous solution containing 1.0 wt.% of MPD for 3-5 min followed by draining off for 2-5 min to remove excess solution. It was then immersed into hexane solution of TMC of desired concentration (0.1 wt.%) with TBP additive 0.1 wt.% for 60 sec followed by draining off excess solution. The polymerization reaction occurs on the surface of polydopamine coated hollow fiber membrane resulting in the formation of an ultrathin layer of cross-linked co-polyamide. The composite membrane so obtained was cured in hot air circulation at 70-80 °C for 5 min whereby polymer layer attains chemical stability.[36] After heat treatment dry the membrane at room temperature for 2 h and then stored it in DI water until next use. The Table 1 discloses the compositions of aqueous and non aqueous solution and reaction time used for interfacial polymerization.

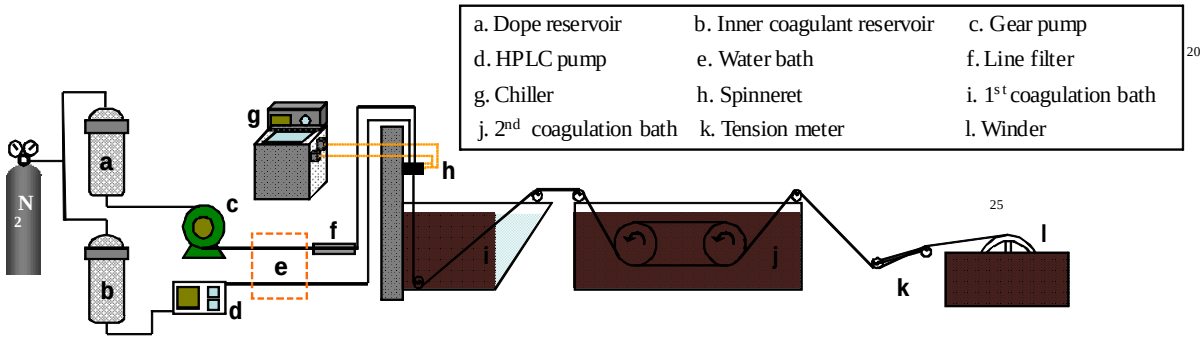

Fig. 1: Schematic diagram of HFM spinning system.

Table 1: Dopamine coating conditions for the preparation of selective layer

Entry	Membrane Code	Dopamine coating	Composition		Reaction Time (Sec)
			MPD/PIP (%w/w)	TMC (%w/w)	
1	PES/PA-M1	0 h	1.0	0.1	60
2	PA without additive- M2	1 h	1.0	0.1	60
3	PA with additive- M3	1 h	1.0	0.1	60

2.2.4. Membrane flux performance

A schematic diagram of the bench-scale PRO setup is shown in Fig. 2. PDA coated thin film composite membranes were evaluated for permeates flux and rejection on a PRO test kit. A high pressure pump was used to transport and pressurize the draw solution that passed through the active surface side of the hollow fiber membrane module. The active layer of the membrane was always facing the draw solution for the PRO tests. Membrane permeate flux (i.e., volumetric flux of water) was determined at predetermined time intervals by measuring the weight changes of the feed tank with a digital mass balance connected to a computer data logging system. Testing was done with NaCl solution at different operating pressures. Hollow fiber membrane module was prepared with effective membrane area was around 7.2 cm^2 and the length of module is around 20.0 cm. A standardized digital conductivity meter of UTV, US was used to measure the salt concentrations in the feed and product water for determining membrane selectivity. The volume of permeate collected was used to describe flux in terms of liter per square meter of active membrane area per hour (L/m^2h). For the details regarding calculations please see the supporting information.

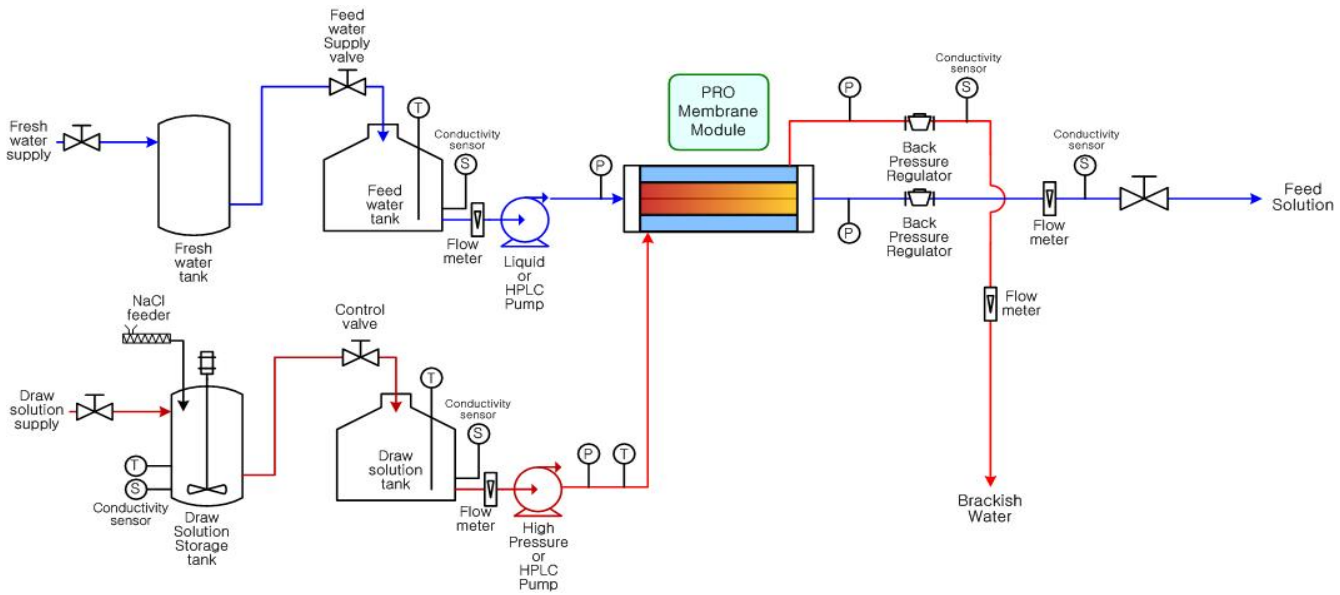

Fig. 2: Pressure retarded osmosis (PRO) testing unit.

2.2.5. Membrane characterization

2.2.5.1. Attenuated total reflection-Fourier transforms infrared spectroscopy (ATR-FTIR)

The PDA coated selective thin film composite membranes were characterized by variable angle attenuated total reflectance Fourier transform infrared (ATR-IR) spectroscopy to elucidate chemical structure of the selective thin film composite membranes. ATR-FTIR spectra were recorded on ALPHA-P Spectrometer with a diamond ATR cell (Bruker) in the range of 600 - 4000 cm^{-1}. A total of 30 scans were performed at a resolution of 4 cm^{-1} with a germanium crystal at temperature of 25±1 °C. A program written for the V2 software from Bruker was used to record the spectra and for the selection of the corresponding backgrounds.

2.2.5.2. Membrane morphology

The performance of composite membranes largely depends on the chemical composition of selective thin film and the morphology of membrane which depends on fabrication parameters controlling kinetics and diffusion rates of the reactants, hydrolysis of reactants, cross-linking and post-treatment. Therefore study of the membrane morphology is highly relevant to understand the membrane performance.

The morphology of membranes was studied by Scanning Electron Microscope (SEM, S-4700, Hitachi) using dried, fractured and gold sputtered samples at a potential of 5–20 kV. The surface topography of membranes was studied by atomic force microscope/Surface Probe Microscope using Nanoman AFM system (Veeco) in tapping mode. Small strip of membranes was placed on specific sample holder and 3 µm × 3 µm areas were scanned. Mean roughness (R_a), root mean square Z values (R_{ms}), and maximum vertical distance between the highest and lowest data points (R_{max}) were used to quantify the surface topology of membranes. The internal structure of selective layer was observed in Transmission Electron Microscope (TEM) (JEOL JEM-2100 TEM) at an accelerating voltage of 200 kV.

2.2.5.3. Water contact angle of membranes

Surface hydrophilicity of membrane substrates was evaluated by contact angle drop shape geometry (DSA100, Germany) using Milli-Q deionized water as the probe liquid at room. To minimize the experimental error, the contact angle was randomly measured at more than 10 different locations for each sample and the average value was reported.

2.2.5.5. Porosity analysis

Membrane effective porosity refers to the volume fraction of the connected voids to the total void volume and may be given by following equation:

$$\varepsilon = \frac{V^{cp}}{V^{v}} \qquad (1)$$

Here ε is membrane effective porosity, V^{cp} and V^{v} are volume of through pores and total void volume.

For the details concerning pore size analysis and calculations please see the supporting information.

3. Result and discussion

3.1. Membrane physicochemical characteristics

3.1.1. ATR-FTIR

Figure 3 presents the FT-IR results for a comparison between the PES substrate and the composite membranes. FTIR spectra displaying peaks at around 1107, 1151, 1243, 1291, 1322, 1487 and 1578 cm^{-1} are characteristics of the PES membrane material. In particular peaks around 1487 and 1574 cm^{-1} are the characteristics of PES. The FTIR spectrum of the PDA coated PES-1 h substrate is composed of bands attributed to both the PDA layer and PES substrates. The peak at 1610 cm^{-1} was attributed to the aromatic rings stretching vibrations and N–H bending vibrations, and the peak at 3400 cm^{-1} was attributed to the catechol –OH groups and N–H groups. After surface coating of PDA, compared with the PES membrane, several new absorption signals appeared and a broad peak between 3600 and 3000 cm^{-1} was attributed to the stretching vibrations of the N–H/O–H and the intensive peak at 1610 cm^{-1} was the overlapped peaks of C–C vibrations of the aromatic ring and the N–H bending vibrations. These changes of the characteristic peaks indicated the existence of PDA on the membrane surface, and the PDA coating was successful. The peak at 1654 cm^{-1} is attributed to stretching vibration of C=O which is formed by the oxidation of the catechol groups into quinine during the self-polymerization.[23,37] In addition the presence of two main peaks around 1670 and 1550 cm^{-1} corresponding to amides I (C=O) and II (N–H) respectively are the indication of the formation of polyamide (PA) thin film.

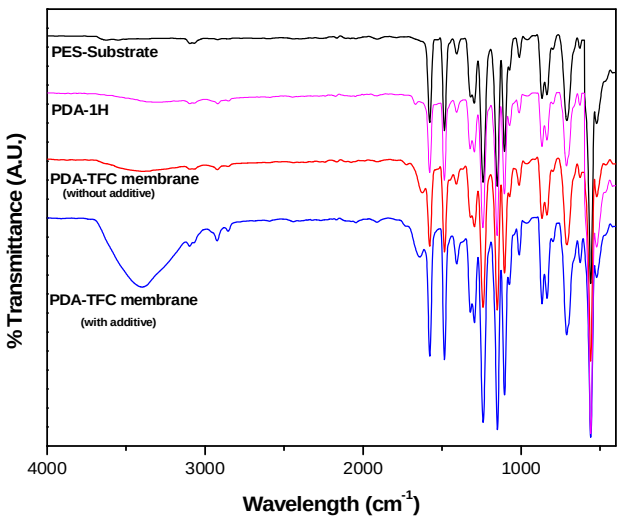

Fig. 3: ATR-FTIR spectra of PES/PA- M1, PDA coated PES-1 h PDA/PA without additive- M2 and PDA/PA with additive- M3 membranes with operation pressure.

3.1.2. Morphological analysis

The morphology of composite membrane was observed in scanning electron microscope. The top and transverse section of composite membrane (Fig. 4) indicates clearly a top thin dense layer (selective layer) and porous thick bottom layer (support layer). Fig. 4a and b shows the SEM images of the selected PES membranes. The polydopamine coated membrane (Fig. 4c) shows dispersed granular surface with visible open pore structures. The thickness of coated membrane is clearly seen in the figure. The cross-sectional morphology of the resultant TFC coated on polydopamine hollow fiber membranes is shown in Fig. 4d. Polyamide membranes dispersed granular surface with visible

open pore structures were shows as a Fig. 4d (TFC membrane). Since the active polyamide layer was synthesized on the outer surface of the polydopamine coated hollow fiber substrate, the structure of the membrane substrate is much different before and after interfacial polymerization. This thin PA layer is the functional selective layer whose nature primarily determines the water permeability and power density of the resulting TFC-PRO membrane. The MPD+TMC PA selective layers formed on PDA coated HF substrates are thinner membrane materials its clearly shown in Fig. 4d. The physico-chemical properties of the intermediate PDA layer may play the most important role in determining the PRO performance of these TFC membranes.

Figure S1 (Supporting Information Fig. S1) illustrates the evolution of colour change with time of the PDA functionalized PES hollow fiber membranes before and after coating with thin film composite polyamide layer. Clearly, the dopamine has successfully self-polymerized and coated on the PES hollow fiber membranes top surface it can be observed that the thickness increases after coating of PDA and it is proved by SEM images after and before coating of PDA as shown in Fig. 4.

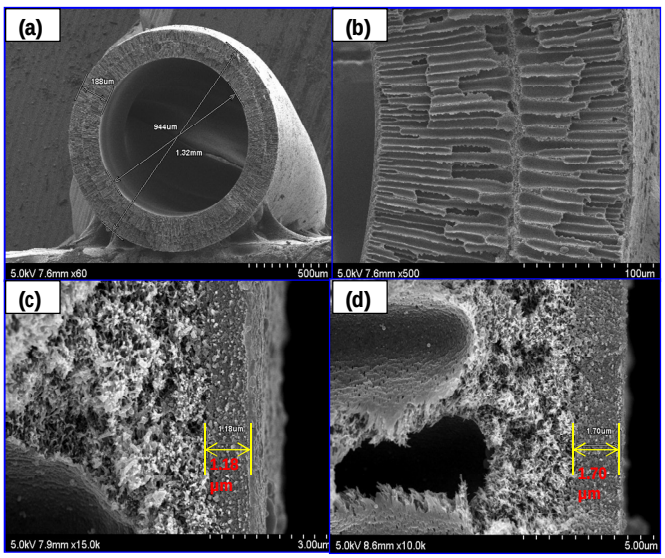

Fig. 4: SEM images of (a and b) PES substrate, (c) after polydopamine coating and (d) interfacial polymerization forming a polyamide (PA) thin film coating with additive.

3.1.3. Surface morphologies of the thin-film layer by AFM

The roughness of the outer surface of the hollow fiber membranes was determined by AFM. Fig. 5 shows the 3-dimensional (3D) micrographs indicating the surface topology of the substrate and the TFC membrane. From the three-dimensional AFM images in Fig. 5, it can be observed that PES substrates coated by PDA before and after thin film composite formation have different top surface roughness. Table 2 summarizes the surface roughness parameters in terms of R_a, R_{ms} and R_{max} for substrate PES, PDA 1 h coated membrane along with TFC membrane. Generally, the modified membranes have improved hydrophilicity, smoothened surface, smaller surface pores and narrower pore size distribution compared to the uncoated substrate.[38-40] These improvements may affect the formation of the selective polyamide layer and influence the PRO performance of the resultant TFC membranes.

With the addition of TBP into the TMC organic solution, the surface morphology of the membrane prepared without TBP addition was changed. The addition of TBP in the TMC organic solution during interfacial polymerization tends to increase the ridge portion of the polyamide TFC membrane.[41] The AFM image of the membrane with no TBP addition shows a ridge-and-valley structure. The membrane with the addition of 0.5 wt.% TBP in the TMC organic solution indicates that the surface of the TFC polyamide film has a broad ridge and a loose structure compared to the membrane without TBP addition.

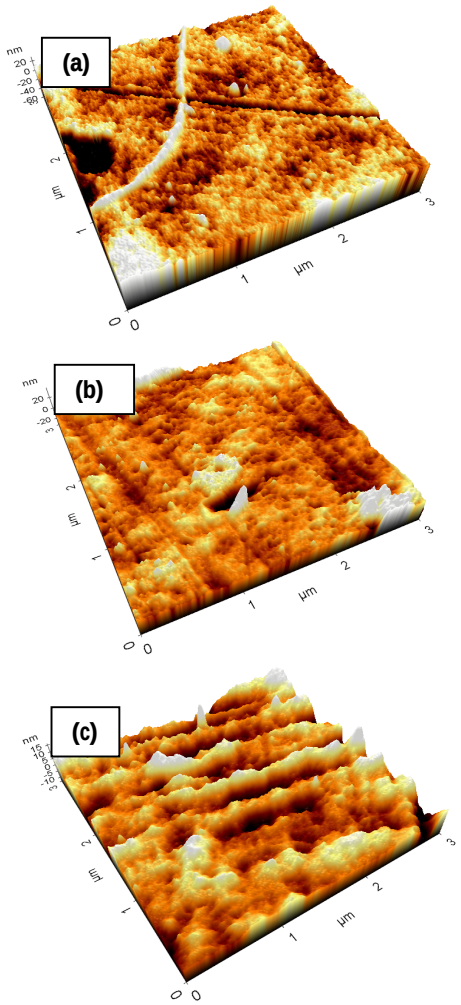

Fig. 5: AFM images of the selected (a) PES/PA- M1, (b) PDA/PA without additive- M2 and (c) PDA/PA with additive- M3 PDA coated hollow fiber membranes.

Table 2: Surface roughness values of the thin film composite membranes

Membranes	R_{ms}(nm)	R_a(nm)	R_{max}(nm)
PES/PA-M1	9.18	7.79	81.13
PA without additive- M2	14.78	11.24	90.3
PA with additive- M3	18.65	13.15	169.6

3.1.4. Transmission Electron Microscopy (TEM)

A more detailed structural characterization is revealed by TEM images, as shown in Fig. 6. Transmission Electron Microscopy is a highly relevant technique to visualize the internal structure of the thin layer of membranes due to its high-resolution power and possibility to achieve contrast between the areas having different chemical structure.[42] The porous polyethersulfone support having a significant proportion of sulfur atoms is vaguely darker than PDA and polyamide layer. In this Figure 6, we provided the surface of hollow fiber membrane after formation of TFC i.e. Fig. 6a, the second Fig. 6b is scan on the scale 0.1 µm and here we found the pores of various sizes. Fig. 6c scans after cutting the hollow fiber membrane to show the TFC layer on the surface of the PES support membrane. The darker part of the skin is almost as thin as in the original membrane and no penetration of the pores of the support by the polymer is observed (Fig.6c). The bright and dark regions in the TEM images arise from the difference in electron densities between the PDA main chains and the PA side chains. It may be seen from the micrographs that the amine-dominated interlayer (Figs. 6b and c) fills the cavities of the polyethersulfone support and largely varies in thickness.

3.1.5. Contact angle

Table 3 shows the water contact angle of the PES substrate, top surface of PDA coated PES substrates as well as TFC membrane. Consistent with the observation after coating of PDA decreases the contact angle, but after TFC coating results in a rapid decrease in water contact angle from 108° (±5) of the PES to 51° (±4). Furthermore, dopamine may penetrate into the pores inside the substrate and attach onto the pore wall via self-polymerization reaction during the PDA modification process, which can enhance their hydrophilicity.[43] After interfacial polymerization with and without additives the contact angle results are shown in Table 3.

3.1.6. Pore size analysis

To measure the effective porosity, the gas is pressurized over the fluid saturated membrane. The fluid from the largest pore is blown out first and gas starts flowing through the membrane. This point is called bubble point and diameter of the pore is known as bubble point diameter. As the gas pressure is increased continuously, smaller pores get open subsequently and flow of gas increases. At the stage when gas flows through all the pores present in the membrane at specified pressure range, the flow of gas through wet membrane equals to the flow of gas through dry membrane. At this point the diameter of the pores is noted as smallest pores. The pores present in the membrane lies between largest and smallest pores. The porosity analysis of the membrane has been given in Table 4 and in Fig. 7.

It is seen that the porosity of the membrane increases after addition of TBP additive at the time of interfacial polymerization in the organic solution. Further membrane prepared from organic solution without additive and only PES/PA contained small pores compared to those prepared from organic solution contained additive. It means that additive content in membrane preparation solution strongly influence the porosity of the membrane.

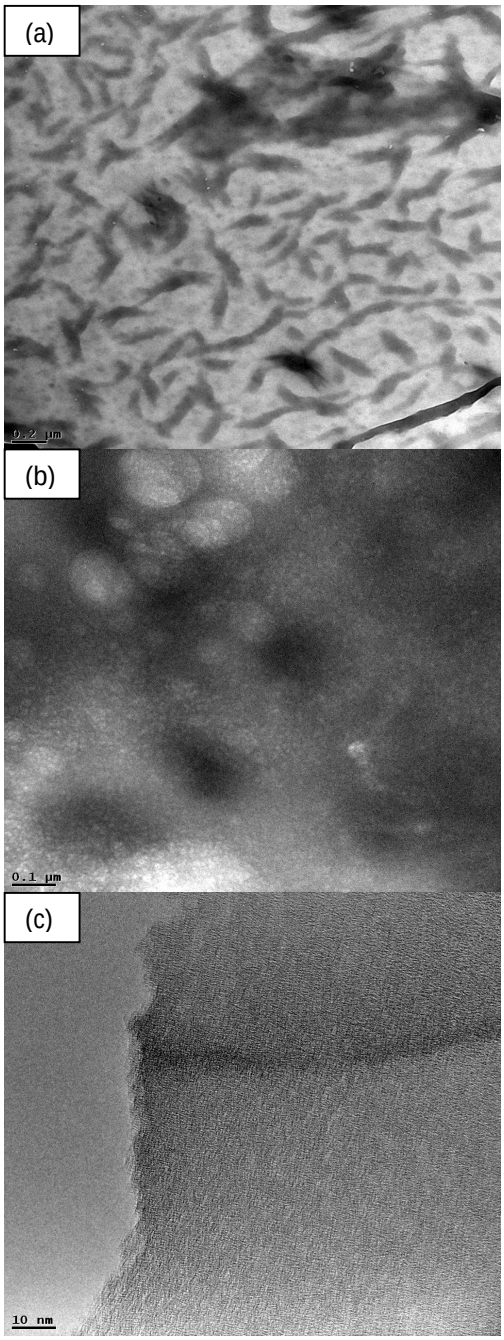

Fig. 6: TEM images of the selected (a) PES/PA- M1, (b) PDA/PA without additive- M2 and (c) PDA/PA with additive- M3 PDA coated hollow fiber membranes.

Table 3: Contact angle measurement results of membranes

Entry	Membrane name (time)	Contact angle (°)
1	PES substrate	108 ±5
2	PES/PA-M1	73 ±4
3	PA without additive- M2	57 ±4
4	PA with additive- M3	51 ±4

Table 4: Porosity analysis of the PES/PA-M1, PA without additive- M2 and PA with additive- M3membranes

Membrane Parameters	PES/PA-M1	PA without additive - M2	PA with additive-M3
Smallest pore diameter (µm)	1.33	1.513	1.712
Mean flow pore diameter (µm)	1.782	1.854	2.141
Bubble point diameter (µm)	2.292	2.324	2.512
% Distribution of max. pore flow	74.34	78.54	85.34
Diameter at max. pore flow (µm)	1.521	1.652	1.872

3.2. Membrane performance

3.2.1. Water permeability

Fig. 8 shows that osmotic water flux was increased significantly following modification of the M2 and M3 membranes with and without additives. The hollow fiber membrane module was first compacted with DI water at an applied pressure, ΔP, of 1.0 bar. The applied pressure was changed up to 8 bar. The pure water flux results obtained for the modified membranes were interesting and unexpected. The modified membranes exhibited an increased hydraulic permeability (Fig. 8). The increased permeability of the PDA modified membrane is likely due to the hydrophilization of the support layer at the interface of the PES layer and the polyamide selective layer. By increasing the hydrophilic character of this interface, transport of water from the polyamide layer is more favourable. We presume that water transporting through the now hydrophilic support layer encounters less surface energy resistance than normally associated with an unmodified hydrophobic PES support. This observation is similar to those reported previously, where the PDA modified M2 and M3 membranes exhibited increase in flux.[33] We have clearly observed after adding TBP additives there is tremendous change in flux as shown in Fig. 8. Figure S2 (Supporting Information Fig. S2) shows a snapshot of the MD simulation system. The system consists of two square membranes (3.3 nm long in the x and y directions and 1.5 nm thick in the z direction) separating two KCl solutions of different concentrations. The membrane atoms are located in a face centred cubic fashion in the xy plane. Membrane consists of a semipermeable pore (only water can go through the pore and ions do not go through the pore) of diameter 7 Å at the centre of the membrane.

3.2.2. Salt Rejection

Salt rejection was characterized by keeping the applied pressures up to 8 bar and measuring rejection of 500 ppm NaCl solution using a calibrated conductivity meter. Observed NaCl rejection, R, was determined from the difference in feed (C_f) and permeate (C_p) salt concentrations,

$$R = 1 - C_p / C_f \qquad (6)$$

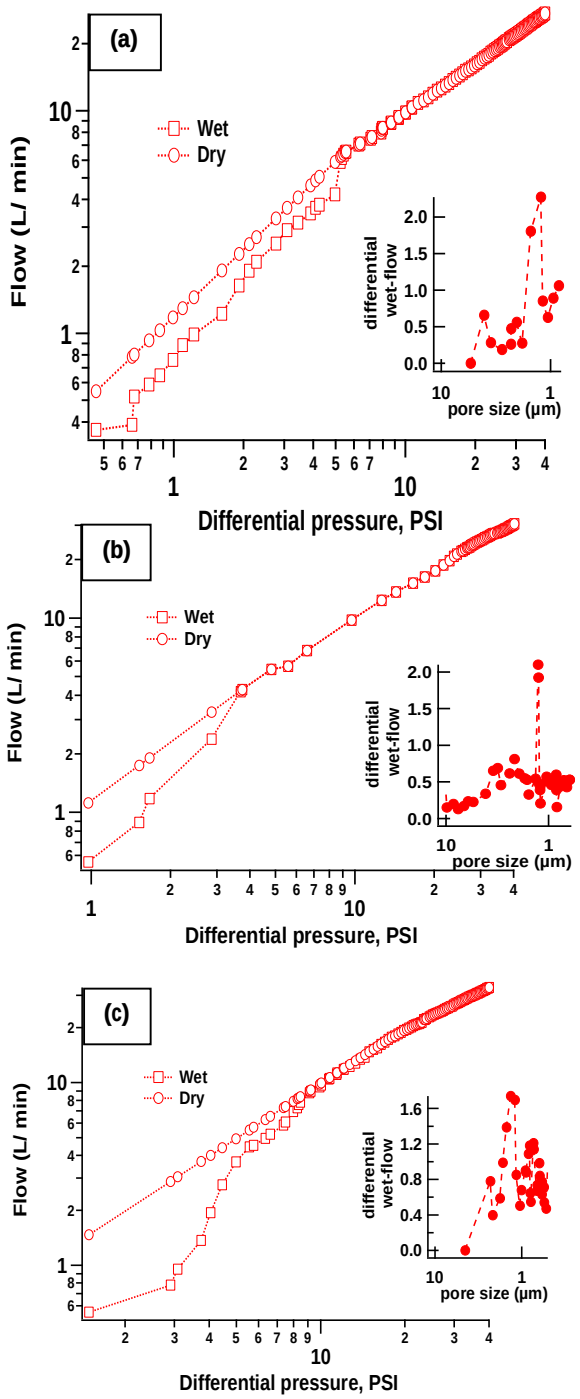

Fig. 7: Pore size distribution in the selected (a) PES/PA- M1, (b) PDA/PA without additive- M2 and (c) PDA/PA with additive-M3 PDA coated hollow fiber membranes.

The rejection values for each sample are the average of three different measurements collected over a ~10 min period. The temperature of the system was maintained at 25 °C throughout the experiment. Fig. 8 shows the variation in pure water flux and Fig. 9 show the variation in salt rejection (500 ppm) with operation pressure. With the addition of additive in MPD solution

the NaCl rejection by the polyamide thin film increases. The maximum NaCl rejection and flux was 98.23% and 26.32 L/m^{2}h respectively by using PA with additive- M3 on 1 h coated PDA hollow fiber membrane was observed. The thin film displayed high free volume and was therefore expected to display high flux. In the case of our experimental results shows that increase in flux by using MPD as monomer crosslinked after addition of additive with TMC could be due to the increased free volume within the thin film.

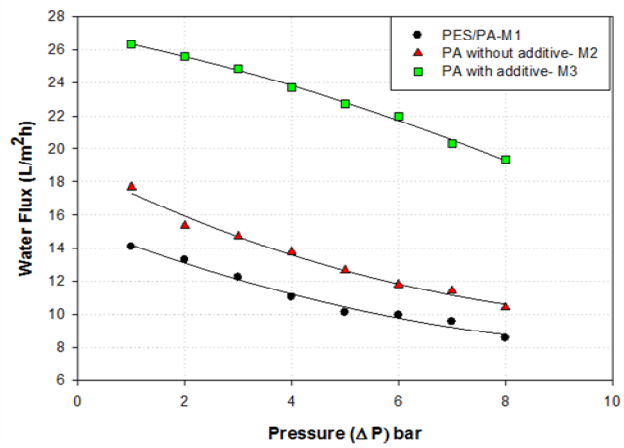

Fig. 8: Variation in pure water flux using PES/PA- M1, PDA/PA without additive- M2 and PDA/PA with additive- M3 membranes with operation pressure.

3.3. Water flux and power density

The PRO performance of PDA coated TFC (MPD+TMC) before and after addition of additive using 0.6 M NaCl solution as the draw solution and deionized water as the feed solution was tested under PRO modes. The TFC on PES membrane, made before addition of additive shows a poor water flux as low as 5.78 L/m^{2}h under the PRO mode with 1.24 W/m^2 power density. However, the water flux dramatically increases when the TBP additive is added at the time of preparation of PA active layer, and it reaches up to by using PA with additive- M3 on 1 h PDA coated TFC membrane 18.26 L/m^{2}h with 3.9 W/m^2 power density at 8 bar (as shown in Fig. 10 and Fig. 11 respectively).

To evaluate the impact of additive for the formation of PA layer on PDA coated PES hollow fiber membranes for PRO applications, the membranes were tested for osmotic flux in the PRO mode. The PES/PA-M1, PA without additive- M2 and PA with additive- M3 membranes were compared and the results have been shown in figures. The additive included PDA modified PA membranes exhibited substantial flux improvement, indicative of an increased hydrophilicity of the membrane support layer. This increased hydrophilic nature promotes water transport through the support layer and to the interior interface of the polyamide layer.[33]

3.4. Effect of tributyl phosphate (TBP) additive on the performance of hollow fiber membranes

As we seen after adding the tributyl phosphate (TBP) additive at the time of TFC membrane preparation there is tremendous effect towards membranes performances. The experimental results indicated that after addition of TBP additive; the retention properties of composite membrane are different; the certain concentration of TBP additives can be retained in the membrane properties of the same circumstances, so that membrane water flux increased. The PA with additive- M3 membrane made from a PDA coating time-1 h shows the highest water permeability and power density. A relatively high flux polyamide TFC membrane could be fabricated by adding additive in organic solution. The rejection levels were similar for all of the membranes, at 97.5–98.2%. For the membranes using TBP as an additive in the organic solution, an increase in the water flux was observed with no significant loss of salt rejection.

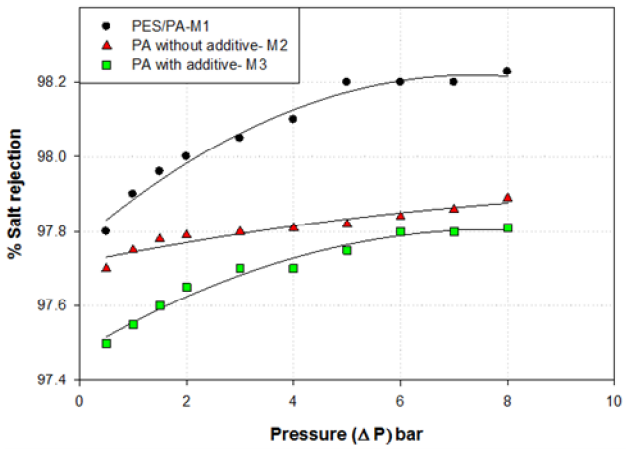

Fig. 9: Variation in salt rejection using PES/PA- M1, PDA/PA without additive- M2 and PDA/PA with additive- M3 membranes with operation pressure.

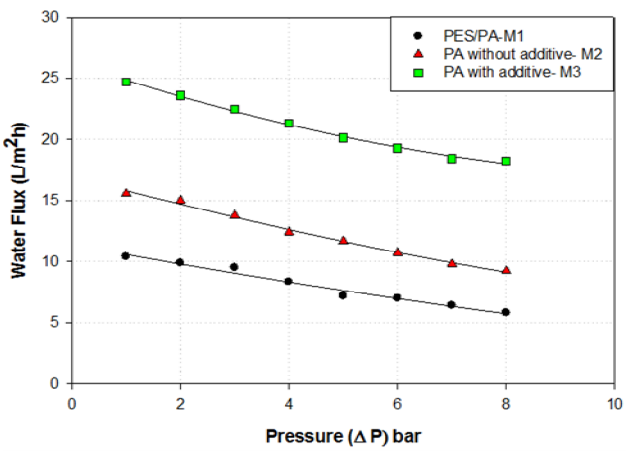

Fig. 10: Variation in water flux using PES/PA- M1, PDA/PA without additive- M2 and PDA/PA with additive- M3 membranes with operation pressure.

The polyamide film formation is described to take place in three steps: embryonic film formation which is a fast process

followed by slow down in polymerization depending upon the permeability of the initial film formed; finally shifting to a diffusion controlled process. The initial layer formed during the embryonic film formation is the actual barrier layer controlling the separation characteristics of the thin film and divides the film in two regions; each region is rich in one type of monomer and end group. In the diffusion controlled step film growth takes place until the monomers diffusing through the film get consumed by other monomers and/or unreacted functional groups of the film.[44] Furthermore membranes prepared using 1.0% concentration of MPD solutions with 0.1% TMC concentration exhibited higher flux with high power density. The interfacial polymerization between MPD and TMC occurs in the organic side; the reaction is diffusion-controlled and exists in a self-limiting phenomenon. The reaction time plays an important role in determining the extent of polymerization, and thereby the cross-linking degree and thickness of top skin layer as well as the resulting membrane performance.[45] The power densities of the modified membranes are presented in Fig. 11. The highest power density of 3.9 W/m^2 was obtained from the PDA/PA modified with additive (M3) membrane at 8 bar operating pressure, which is noticeably higher than the reported asymmetric TFC membrane 1.5 W/m^2 at 11 bar pressure.[46]

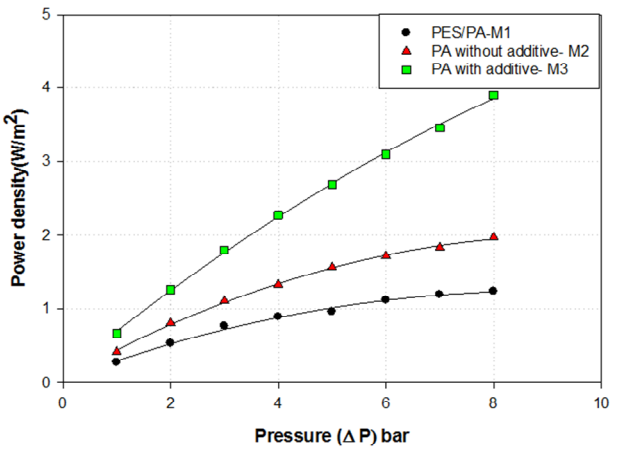

Fig. 11: Variation in power density using PES/PA- M1, PDA/PA without additive- M2 and PDA/PA with additive- M3 membranes with operation pressure.

4. Conclusions

In this study, we demonstrate for the first time fabrication of a TFC membrane via interfacial polymerization on a PDA coated hollow fiber membrane with tributyl phosphate (TBP) as an additive in the organic solution of monomer to increase the water flux and power density. Thin crosslinked aromatic polyamide barrier layer films as well as support membranes were characterized by ATR-FTIR spectroscopy, SEM, AFM, TEM and pore size analysis, versus water permselectivity and power density. These all prepared membranes demonstrated higher flux and high power density values when convection was present as a result of thrilling. Overall, these results suggest that the surface patterns induced hydrodynamic secondary flows at the membrane-feed interface which were effective in increasing power density. This improved fabrication process can provide a new paradigm for the preparation of high performance TFC-PRO membranes. The modified membranes must possess tough mechanical properties to withstand the compression, trim and elongational stresses during the high pressure PRO process without showing structural damage and sacrificing much water flux. The support membrane pore morphology and hydrophilicity have a strong impact on a membrane's performance in osmotically driven processes. Our results show that coating on the polyethersulfone hollow fiber support layer containing polydopamine and polyamide causes an increase in water flux in PRO mode in osmotically driven processes and an increase in water flux during addition of additive and applied pressure driven PRO tests.

Acknowledgements

This work was conducted under the framework of Research and Development Program of the Korea Institute of Energy Research (KIER) (B3-2441-02).

Notes and references

Greenhouse Gas Research Center,
Korea Institute of Energy Research (KIER), 71-2 Jang-dong, Yuseong-gu, Daejeon-305343, Republic of Korea,
Tel.: +82-42-860-3647
Email address: hklee@kier.re.kr (Hyung-Keun Lee)

1. M. Elimelech and W.,A. Phillip, *Science*, 2011, **333,** 712-717.
2. M. Elimelech and R. McGinnis, *Membr. Technol.*, 2009, **4,** 10-11.
3. Q. Schiermeier, *Nature*, 2008, **452,** 260-261.
4. S. Patel, *Power*, 2011, **155,**13-14.
5. R. L. McGinnis and M. Elimelech, *Environ. Sci. Technol.*, 2008, **42,** 8625-8629.
6. R. J. Aaberg, *Refocus*, 2003, **4,** 48-50.
7. *A new spin on forward osmosis*, Water Desalination Report, Houston, 2012, **48**.
8. X. Song, Z. Liu and D.,D. Sun, *Energy Environ. Sci.* 2013, **6,** 1199-1210.
9. C. Klaysom, T. Y. Cath, T. Depuydt and I. F. J. Vankelecom, *Chem. Soc. Rev.*, 2013, **42,** 6959-6989.
10. J. T. Arena, B. McCloskey, B. D. Freeman and J. R. McCutcheon, *J. Membr. Sci.*, 2011, **375,** 55-62.
11. A. Tiraferri, N. Y. Yip, W. A. Phillip, J. D. Schiffman and M. Elimelech, *J. Membr. Sci.*, 2011, **367,** 340-352.
12. J. Wei, C. Qiu, C. Y. Tang, R. Wang and A. G. Fane, *J. Membr. Sci.*, 2011, **372,** 292-302.
13. S. Chou, L. Shi, R. Wang, C. Y. Tang, C. Qiu, A. G. Fane, *Desalination*, 2010, **261,** 365-372.
14. R. Patel, W. S. Chi, S. H. Ahn, C. H. Park, H. K. Lee and J. H. Kim, *Chem. Eng. J.*, 2014, **247,** 1-8.
15. J. L. H. Chau, A. Y. L. Leung and K. L. Yeung, *Lab Chip*, 2003, **3,** 53-55.
16. S. M. Kwan and K. L. Yeung, *Chem. Commun.*, 2008, 3631-3633.
17. K. L. Yeung, S. M. Kwan and W. N. Lau, *Top. Catal.*, 2009, **52,** 101-110.
18. C. Yuan, Q. Liu, H. Chen and A. Huang, *RSC Adv.*, 2014, **4,** 41982-41988.
19. M. G. Buonomenna, *RSC Adv.*, 2013, **3,** 5694-5740.
20. J. E. Cadotte, R. J. Petersen, R. E. Larson and E. E. Erickson, *Desalination*, 1980, **32,** 25-31.

21. R.E. Larson, J.E. Cadotte and R.J. Petersen, Desalination 1981, **38,** 473-483.
22. P. G. Ingole, W. Choi, K. H. Kim, H. D. Jo, W. K. Choi, J. S. Park and H. K. Lee, *Desalination*, 2014, **345,** 136-145.
23. L. Shi, S. R. Chou, R. Wang, W. X. Fang, C. Y. Tang and A. G. Fane, *J. Membr. Sci.*, 2011, **382,** 116-123.
24. F. Y. Li, Y. Li, T. -S. Chung, H. Chen, Y. C. Jean and S. Kawi, *J. Membr. Sci.*, 2011, **378,** 541–550.
25. S. H. Yun, P. G. Ingole, K. H. Kim, W. K. Choi, J. H. Kim and H. K. Lee, *Chem. Eng. J.*, 2014, **258,** 348-356.
26. K. H. Kim, C. H. Hyung, P. G. Ingole, J. H. Kim and H. K. Lee, *J. Appl. Poly. Sci.*, 2014, **131,** DOI: 10.1002/app.39711.
27. A. Rahimpour, M. Jahanshahi, N. Mortazavian, S. S. Madaeni and Y. Mansourpanah, *Appl. Sur. Sci.*, 2010, **256,** 1657-1663.
28. H. Lee, N. F. Scherer and P. B. Messersmith, *Science*, 2006, **103,** 12999-13003.
29. H. Lee, Y. Lee, A. R. Statz, J. Rho, T. G. Park and P.B. Messersmith, *Adv. Mater.*, 2008, **20,** 1619-1623.
30. H. Lee, S. M. Dellatore, W. M. Miller and P. B. Messersmith, *Science*, 2007, **318,** 426-430.
31. L. P. Zhu, J. H. Jiang, B. K. Zhu and Y. Y. Xu, *Colloids Surf. B.*, 2011, **86,** 111-118.
32. J. T. Arena, B. D. McCloskey, B. D. Freeman and J. R. McCutcheon, *J. Membr. Sci.*, 2011, **375,** 55-62.
33. P. G. Ingole, W. Choi, K. H. Kim, C. H. Park, W. K. Choi and H. K. Lee, *Chem. Eng. J.*, 2014, **243,** 137-146.
34. K. H. Kim, P. G. Ingole, J. H. Kim and H. K. Lee, *Polym. Adv. Technol.*, 2013, **24,** 997-1004.
35. K. H. Kim, P. G. Ingole, J. H. Kim and H. K. Lee, *Chem. Eng. J.*, 2013, **233,** 242-250.
36. P. G. Ingole, H. C. Bajaj and K. Singh, *Desalination*, 2012, **305,** 54-63.
37. L. P. Yang, S. L. Phua, J. H. Teo and X. H. Lu, *ACS Appl. Mater. Interfaces*, 2011, **3,** 3026-3032.
38. P. G. Ingole, K. Singh and H. C. Bajaj, *Ind. J. Chem. Technol.*, 2011, **18,** 197-206.
39. P. G. Ingole, H. C. Bajaj and K. Singh, *RSC Adv.*, 2013, **3,** 3667-3676.
40. P. G. Ingole, K. Singh and H. C. Bajaj, *Desalination*, 2011, **281,** 413-421.
41. I. -C. Kim, B. -R. Jeong, S. -J. Kim and K. -H. Lee, *Desalination*, 2013, **308,** 111-114.
42. V. Freger, J. Gilron and S. Belfer, *J. Membr. Sci.*, 2002, **209,** 283-292.
43. D. J. Miller, D. R. Paul and B. D. Freeman, *Polymer*, 2014, **55,** 1375-1383.
44. R. Nadler and S. Srebnik, *J. Membr. Sci.*, 2008, **315,** 100-105.
45. P. W. Morgan and S. L. Kwolek, *J. Polym. Sci. Part A: Polym. Chem.*, 1996, **34,** 531-559.
46. X. Li, S. Zhang, F. Fu and T. -S. Chung, *J. Membr. Sci.*, 2013, **434,** 204-217.

